Development of a new method for the detection of illicit materials based on the active interrogation method and photoneutron spectrometry

Clement Besnard Vauterin, Valentin Blideanu, Benjamin Rapp

Development of a new method for the detection of illicit materials based on the Active Photon Interrogation Method and photo-neutron spectrometry

C. Besnard-Vauterin[1,*], V. Blideanu[1], and B. Rapp[1]
[1]Université Paris-Saclay, CEA, List, Laboratoire National Henri Becquerel (LNE-LNHB)
F91120, Palaiseau, France
(*) clement.besnardvauterin@cea.fr

***Abstract*—The detection of illicit materials is a critical task in the field of homeland security, as international trade has contributed to the increase of smuggling activities. Non-intrusive on-site inspections are crucial in this context, but the current active interrogation methods have limitations. Neutron-induced reactions have been used, but the measurement of gamma spectra is complex due to background noise. Active photon interrogation methods have also been overlooked but they are currently limited to actinides detection using photo-fission reactions. This work presents a novel method for the detection of illicit materials based on active photon interrogation and photo-neutron spectrometry. This approach extends the application of active photon interrogation by including the detection of conventional explosives, narcotics, and chemical weapons based on the use photo-nuclear reactions to determine the content of light elements such as nitrogen, oxygen, and carbon. Monte-Carlo codes are the main tool used to simulate this process for the application need. However, because of the lack in the present literature of measured neutron spectra, the experimental validation of the simulations is not straight forward. At present, benchmarking the Monte-Carlo codes seems to be the sole option for testing their ability to accurately simulate photo-neutron production and spectra for the nuclear reactions of interest. Simultaneously, we designed a test bench based on a linear accelerator to generate photons, induce photo-nuclear reactions, and acquire photo-neutron spectra. This study on the fundamental aspects of photo-neutron production lays the groundwork for a promising new detection method for illicit materials.**

***Keywords*—Homeland security, neutron spectrometry, photo-nuclear, photo-neutron, Monte Carlo simulation, CBRNE.**

I. Introduction

In the field of material detection by non-intrusive on-site inspection, the existing techniques can be divided into two families depending on the exploring particles used. Neutron-induced reactions can be used to detect illicit materials in containers (the so-called active neutron interrogation method), using in particular the associated particle technique (APT) [1, 2]. In this case, detection is based on the measurement of gamma radiation produced by neutron-induced reactions (namely inelastic scattering, capture). However, the precise measurement of gamma spectra is generally complex due to the experimental conditions, being often characterized by a high level of gamma background. In the case of the use of photons, the method is called active photon interrogation (API) and is currently used only for threats related to nuclear materials based on the actinide detection using photo-fission reactions and spectrometry of gammas emitted subsequent to the decay of radioactive fission fragments [3].

Our work extends the applicability of traditional API techniques by the development of a novel method, allowing for the first time the detection of light elements such as nitrogen, oxygen and carbon present in illicit materials (conventional explosives, narcotics and chemical weapons) (see Fig. 1), based on active photon interrogation associated to photo-neutron spectrometry. This new method overcomes the difficulties related to gamma-ray spectrometry on which the neutron interrogation is based [4]. In addition, compared to the active neutron interrogation method, this new technique has the advantage that photons are much more penetrating than neutrons for most materials and therefore less subject to scattering and attenuation.

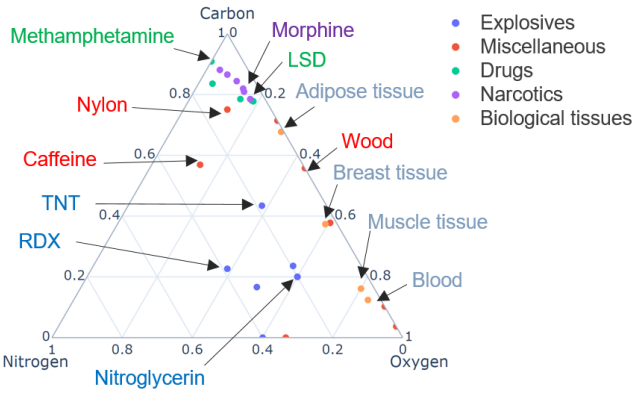

Fig. 1. Triangle of normalized proportions of carbon, nitrogen and oxygen for different materials.

The method presented in this paper for the detection of illicit materials based on the active photon interrogation and photo-neutron spectrometry involves inducing photo-nuclear reactions on light nuclei using ideally mono-energetic photons, with energies above the reaction threshold of about 10 MeV for nitrogen isotopes. This leads to nuclear excitation and subsequent emission of neutrons. The measurement of their spectra allows the identification of the emitting nuclei, and

potentially determine their quantity. The existence of energy levels in nuclei and their low density for light nuclei, gives to the energy spectra of the emitted photo-neutrons the particularity of presenting distinctive peaks at well-known energies.

Among the existing photon sources suitable for this purpose, compact single and dual energy sources with energies above 10 MeV can be obtained namely based on low-energy proton induced resonance reactions, as for example ^{7}Li(p,γ)^{8}Be at 441 keV . These sources are however multi-directional with low effective photon intensities in a given solid angle thus significantly degrading the signal over noise ratio. Another approach, which avoids this limitation while being simpler to set up given the higher availability of the required equipment, consists of using a source of photons produced by an electron linear accelerator (LINAC). However, the bremsstrahlung photons produced in this way do not meet the conditions mentioned above relating to their energy spectrum, which is in this case continuous. Therefore, the implementation of this method requires a special treatment in order to select in the total spectrum of the detected neutrons generated in photo-nuclear reactions by all photon energies, the events associated with a given energy of the photon. This approach, known as the photon tagging method, can be implemented experimentally by using additional equipment but this requires the deployment of a complex and non-compact system for electron spectroscopy and electron-neutron coincidence electronics. Our new approach intends to overcome these limitations. The selection of contribution from photons in a well-defined energy range can be achieved by subtracting two neutron spectra induced by bremsstrahlung photon beams created by electrons of close energies. Furthermore, a deep learning-based method has been developed and successfully tested for the identification of the signatures from specific light elements in the simulated complex photo-neutron spectra from irradiation of compound materials and to extract their respective contributions.

II. Methods

As there is a large reliance on Monte-Carlo methods for the above-mentioned application, especially for establishing the training data sets for the neural networks, the capabilities of the existing codes to accurately simulate the photo-nuclear reactions and a good understanding of physics involved becomes crucial and justifies the need for intercomparisons and benchmarks. The first step of the work described in the present paper was dedicated to the comparison of the photo-neutron energy spectra calculated by the main Monte-Carlo codes used by the community: FLUKA [5], GEANT4 [6], MCNP6.2 [7] and PHITS3.27 [8]. On the other hand, due to the lack of measured neutron spectra in the existing literature, experimental validation of these simulations is challenging. Therefore, benchmarking Monte-Carlo codes appears to be the only viable option to accurately test their capabilities in simulating photo-neutron production. In this study, we analyzed the agreement between Monte-Carlo codes tested for calculated photo-neutron spectra from different nuclei covering a wide range of mass numbers. Based on assumptions derived from photo-nuclear reaction theory, our analysis allowed us to thoroughly test the performance of the codes for this physics case. In order to focus the study on the physics of the photo-nuclear reactions, a simple simulation geometry has been used to calculate with Monte-Carlo codes the photo-neutron spectra and production rates. The geometry consists of a vacuum sphere containing a cylindrical target of 1 mm thickness and 1 cm in diameter. The 1 mm thickness has been chosen as a good compromise in order to increase the rate of photo-nuclear reactions occurring in the target while minimizing the probability of the secondary reactions induced by the particles primary produced by the impinging beam. The target is uniformly irradiated with a parallel 20 MeV photon beam with 1 cm diameter. This photon energy has been chosen in order to ensure a significant photo-nuclear reaction cross-section for most of the elements. Considered materials ranges from beryllium to lead and include carbon, oxygen and nitrogen as elements of particular interest for the application of illicit material detection.

The second step consists in the development of a test bench based of a Varian TrueBeam® medical electron LINAC available in our laboratory to study photo-neutron spectra from the reactions induced on different materials by photons with a continuous energy spectrum up to 20 MeV. A preliminary feasibility and optimization study based on simulations has been performed for the test bench from the point of view of the target, collimation, and detector shielding, considering the fully modeled geometry of the medical accelerator. Neutron spectra from the irradiation of tungsten were measured using a passive Bonner sphere spectrometry system associated to dedicated unfolding techniques. Tungsten has been selected in order to allow quick testing of the simulation capabilities, since this material has a high cross-section for photo-nuclear reaction and consequently the photo-neutron production rate is higher than in the case of light elements. Reasonably low statistical uncertainties for both measured and simulated neutron spectra can therefore be achieved in relatively short times. Comparison of the measured spectra with the results from Monte-Carlo simulations, accurately reproducing experimental conditions, was performed to strengthen the validation of the Monte-Carlo simulation code selected as main tool for further development of the new illicit materials detection method.

III. Results and Discussions

A. Simulation of photo-neutron emission by light nuclei

1) Monte-Carlo codes benchmark for photo-neutron energy spectra

As there are no usable experimental neutron spectra available in the literature allowing the comparison with the Monte-Carlo simulations, the energy conservation aspect is the only indicator available to check the consistency of the simulated spectra. According to the energy conservation law, the expected energy of the photo-neutron can be calculated from Eq. 1 for each excited energy level of the residual nucleus left after the emission of one neutron.

$$E_n = \frac{E_\gamma - E_{thres} - E_{state}}{1 + A_{residual}^{-1}} \quad (1)$$

Where E_γ is the incident photon energy, E_{thres} is the reaction threshold, E_{state} is the energy of the excited state of the residual nucleus (being equal to 0 for the ground state, hereafter abbreviated to g.s.) and A its mass number.

In the present study, carbon was considered as one of target materials, with natural isotopic composition (98.9% of ^{12}C and 1.1% of ^{13}C) and a density of 2 g/cm^3. Figure 2 displays the emitted photo-neutron spectrum from natural carbon when irradiated by 20 MeV photons, calculated by the Monte-Carlo codes considered in this study. A series of well-defined peaks are observed. For the channel ^{12}C(γ,n)^{11}C$_{g.s.}$, a photo-neutron peak is expected at around 1.24 MeV (see Table I) and is accurately reproduced by all codes considered here, with the exception of PHITS3.27. The first excited level of the residual ^{11}C is at 2 MeV ± 0.4 keV. The channel ^{12}C(γ,n)^{11}C$_{1st}$ therefore requires a photon energy of at least 20.74 MeV when considering the reaction threshold of 18.72 MeV, which exceeds the incident photon energy considered in this study. Thus, no signature from excited states of the residual ^{11}C is found in the simulated photo-neutron spectra. Peaks at higher energies are signature of various ^{13}C(γ, n)^{12}C channels, leaving the residual ^{12}C in the ground-state or in the first few low-lying excited states. The corresponding excitation energies are reported in Table II, along with the associated neutron peak energies. FLUKA, GEANT4 and MCNP6.2 all reproduce the peak corresponding to the ground state as well as the first and second excited states of the residual nucleus, although peak intensities may differ by up to an order of magnitude. These peak intensities are roughly a factor of 100 lower than those for ^{12}C(γ, n)^{11}C reflecting the much lower abundance of ^{13}C in natural carbon, even though the cross-section of the photo-nuclear reaction in the case of ^{13}C is 2.4 higher. The photo-neutron peak at 3.88 MeV is only present in the spectra calculated by MCNP6.2 and GEANT4. Additionally, MCNP6.2 seems to predict two other peaks at around 6 MeV and 8.5 MeV that cannot be associated to the ^{13}C(γ, n)^{12}C reaction.

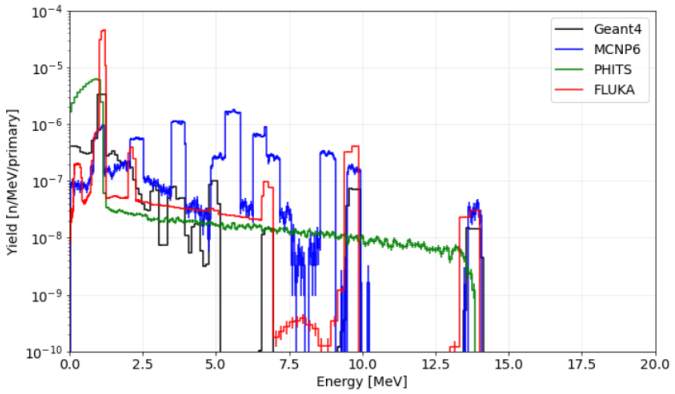

Fig. 2. Simulated energy spectra of neutrons emitted from the irradiation of natural carbon target with 20 MeV photons.

TABLE I
EXPECTED PHOTO-NEUTRON ENERGIES FROM THE ^{12}C(γ, n)^{11}C REACTION

Energy levels of ^{11}C (MeV± keV)	Photo-neutron energy (MeV)
g.s.	1.24

TABLE II
EXPECTED PHOTO-NEUTRON ENERGIES FROM THE ^{13}C(γ, n)^{12}C REACTION

Energy levels of ^{12}C (MeV± keV)	Photo-neutron energy (MeV)
g.s.	14.06
4.439 ± 0.21	9.79
7.654 ± 0.19	6.83
9.641 ± 5	4.99
9.870 ± 60	4.78
10.847 ± 4	3.88
11.836 ± 4	2.97
12.710 ± 6	2.16
13.316 ± 20	1.60
14.019 ± 5	0.90

Special attention has been given to the neutron spectrum from nitrogen irradiation as this element can be used as marker allowing to detect conventional explosives, narcotics and drugs and some chemical weapons with, notably, the emergence of new compounds related to opioid attacks. In this case also, natural nitrogen composition with 99.6 % of ^{14}N and 0.4 % of ^{15}N was used. The density was chosen to be of 1 g/cm^3 in order to speed-up the calculations by artificially increasing the neutron production rate. Both ^{14}N and ^{15}N have very close neutron binding energies of respectively 10.55 MeV and 10.83 MeV. For ^{13}N (residual nucleus from the ^{14}N(γ,n)^{13}N reaction), the ground state predicts a photo-neutron at 8.92 MeV and the first four excited levels photo-neutrons at 6.58 MeV, 5.52 MeV, 5.48 MeV and 2.87 MeV as reported in Table III. Again, the spectra calculated by all codes but PHITS3.27 are showing peaks at these expected energies. It is worth noting that MCNP6.2 also predicts a photo-neutron peak at around 3.75 MeV which can be potentially explained as corresponding to the ^{14}N(γ,pn)^{12}C reaction channel. The MCNP6.2 peaks found at energies higher than 9.5 MeV appear to be beyond the maximum energy allowed by the kinematics of (γ,n) reaction.

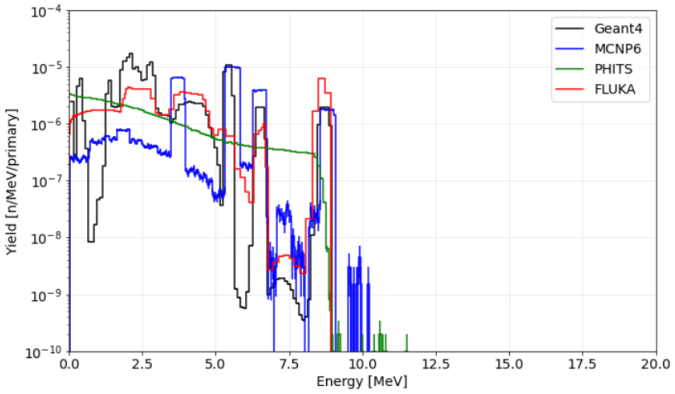

Fig. 3. Simulated energy spectra of neutrons emitted from the irradiation of natural nitrogen target with 20 MeV photons.

TABLE III
EXPECTED PHOTO-NEUTRON ENERGIES FROM THE $^{14}N(\gamma,n)^{13}N$ REACTION

Energy levels of ^{13}N (MeV± keV)	Photo-neutron energy (MeV)
g.s.	8.92
2.3649 ± 0.6	6.58
3.502 ± 2	5.52
3.547 ± 4	5.48
6.364 ± 9	2.87
6.886 ± 8	2.38
7.155 ± 5	2.13

These results show that the shape of the photo-neutrons spectra is strongly influenced by nuclear levels structure for light target elements. Significant differences in how this effect is handled by the various codes were identified, with an extreme behavior in the case of PHITS3.27 for which physics models and data libraries available at the time of the calculations in the distribution package do not account at all for this effect.

2) Intercomparison on total neutron production cross-sections using several Monte Carlo codes and TALYS

While experimental neutron differential distributions in energy and/or angle are rather scarce in the literature, integrated cross section data are more abundant. Thus, while a comparison against experimental data in terms of double-differential cross section is not feasible, a direct comparison against integrated cross sections is possible. To this end, experimental integrated cross section data available through the EXFOR [9] database have been compiled and compared with those extracted from the simulations performed in this work. In addition to the cross-section values estimated from the calculations performed with the Monte-Carlo codes considered here and the experimental data from EXFOR, cross sections calculated with TALYS [10] have been included in the comparison. TALYS is a deterministic code using specially developed and continuously updated reaction models to calculate particle emission probabilities for various reactions. It is used to generate the TENDL nuclear data library which is one of the libraries extensively used by the broad nuclear physics community.

The results are presented in the Figure 4, which displays the cross section as a function of the mass number for the elements considered in this study.

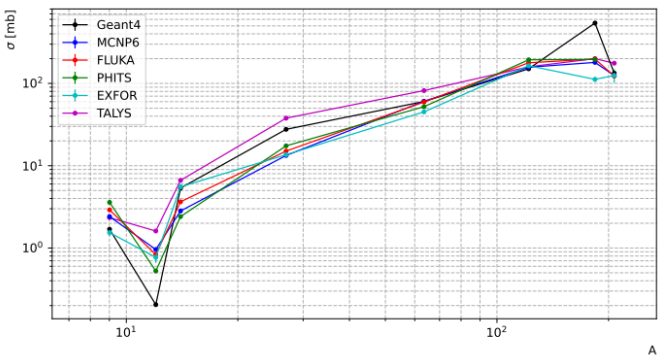

Fig. 4. Simulated and experimental integrated photo-neutron production cross-sections as a function of the atomic mass.

The general trend observed is characterized by an increase of the photo-neutron production cross-section with the mass of the target nucleus, reaching a plateau for heavy elements since no significant increase is observed between tungsten and lead. An exception is to be noted for light elements with the cross-section for carbon being lower than for beryllium. This trend is reproduced by all the Monte Carlo codes tested and by TALYS, however MCNP6.2, FLUKA and PHITS3.27 show better general agreement with the data while GEANT4 and TALYS produce higher cross-sections for light and intermediate mass nuclei. For tungsten all the calculated cross-sections are overestimated. An interesting finding concerns PHITS3.27, which despite showing an inaccurate simulation of the energy spectra of photo-neutrons as discussed in the previous section, is able to reproduce the same trend as the other codes for integrated cross sections. This fact strengthens the importance of the approach of this study, consisting in benchmarks not only in terms of integrated cross-section and production rates, but including also energy differential cross section allowing to better assess the energy spectrum features.

Figure 5 provides a detailed comparison of the cross-section values used by MCNP6.2 and PHITS3.27 concerning photo-neutron production for ^{12}C target nucleus, as a function of the incident photon energy. MCNP6.2 and PHITS3.27 values are in a very good agreement for the cross-section trends for (γ, n) reactions. In addition, the observed trends closely match the experimental data from B. C. Cook *et al.* ([11]) confirming their agreement with measured values.

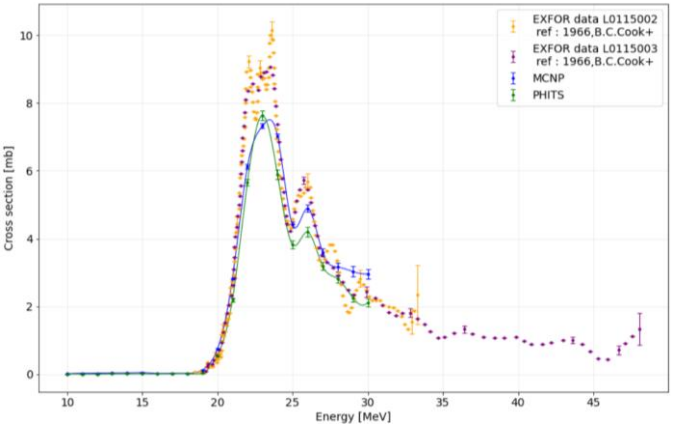

Fig. 5. Cross-section comparison for neutron production in photo-nuclear reactions on ^{12}C between MCNP6.2 and PHITS3.27 as a function of incident photon energy.

Figure 6 highlights contrasting findings in the cross-sections calculated by MCNP6.2 and PHITS3.27 for ^{14}N. While MCNP6.2 results agrees with the cross-sections measured by B. L. Berman et al. ([12]), PHITS3.27 results are closer to the data from J. D. King et al. ([13]). This can be explained by the fact that these two experimental data sets differ significantly in terms of physical process measured, as data from J. D. King refers only to the cross-sections for the (γ,n) channel, while B. L. Berman et al. provides cross-sections including contributions from both (γ, n) and (γ,pn) channels.
Moreover, as data from B. L. Berman et al. suggest, fact also confirmed by other works, the (γ,pn) process is dominant in the

decay of the giant resonance in ^{14}N. This could be an explanation for the difference found in the reaction cross-sections calculated by MCNP6.2 and PHITS3.27 (a factor of ten for 23 MeV photons).

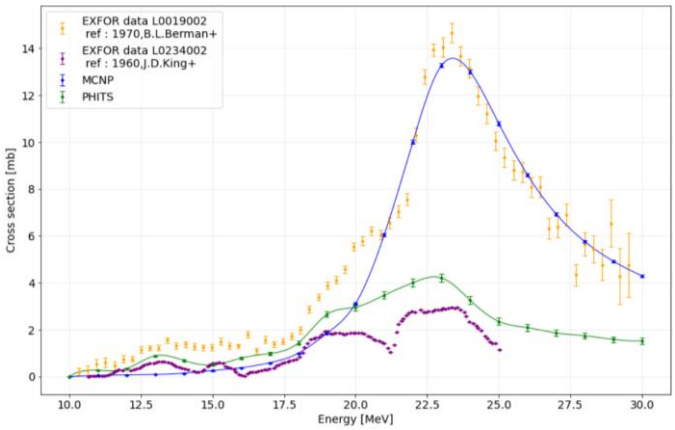

Fig. 6. Cross-section comparison for neutron production in photo-nuclear reactions on ^{14}N between MCNP6.2 and PHITS3.27 as a function of incident photon energy.

The observed discrepancies motivate the importance to be assigned to the underlying neutron emission mechanisms for accurate interpretation and use of cross-section values (either from evaluated libraries or model calculated) in Monte-Carlo simulations. In particular, the observation that MCNP6.2 appears to be in agreement with measured values in terms of total cross-section must be taken with caution since this is achieved without activating the proton physics in the calculations. This leads to the conclusion that the total cross section is calculated by MCNP6.2 without a complete picture of the physics involved but only based on cross-section evaluation using a particular data set. Additional investigation on this matter is essential to delve deeper into this observed phenomenon and gain a comprehensive understanding.

3) MCNP6.2 simulated photo-neutron spectra from molecules of interest for illicit material detection

Based on the findings from the initial study concerning the simulation of photo-neutron energy distributions for natural elements, one can conclude that MCNP6.2 allow a reasonably good accuracy for the purpose of our application in predicting neutron energy values in the outgoing spectra for the materials of interest. This code has been therefore selected for further simulations.

In this context, our focus lies on examining the photo-neutron spectra from various molecules of interest in the context of CBRNE (Chemical, Biological, Radiological, Nuclear, Explosive) risks, when irradiated by 20 MeV photons. Figure 7 illustrates the photo-neutron energy distribution for trinitrotoluene, methamphetamine, and tabun. These molecules correspond respectively to a conventional explosive, a narcotic substance, and a neurotoxic gas hazardous through inhalation or skin contact. Despite the different associated risks, their compositions are very similar, being made of same elements (carbon, nitrogen, and oxygen) only in different proportions.

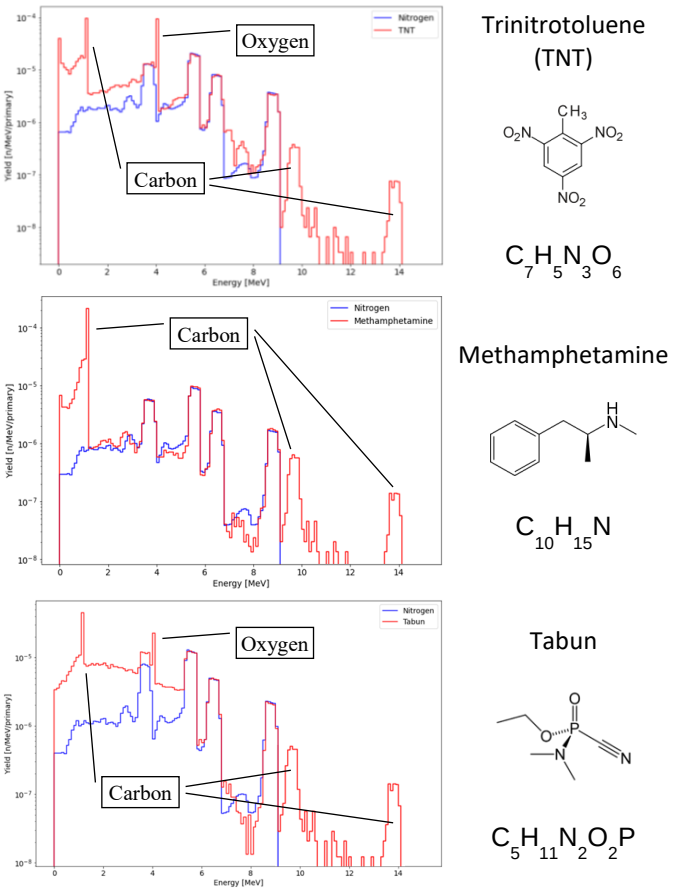

Fig. 7. MCNP6.2 simulated photo-neutron spectra from different molecules when irradiated with 20 MeV photons. The right side of each spectrum provides information on the structure and composition of each molecule.

The blue spectrum on each plot corresponds to the contribution of nitrogen in terms of photo-neutrons being produced. When present, carbon and oxygen contributions are marked with an arrow mark.

One can clearly observe in the simulated spectra the photo-neutron peaks expected at 1.24 MeV and 4.16 MeV, assigned respectively to the ^{11}C and ^{15}O residual nuclei left in their ground states subsequent to (γ,n) reactions on these target nuclei. These contributions can be easily separated from the photo-neutrons emitted in (γ,n) on nitrogen isotopes and thus providing evidence that specific shapes of photo-neutron spectra can be used as signatures for the detection and quantification of illicit materials containing light nuclei such as carbon, nitrogen, or oxygen.

B. Preliminary feasibility studies for the new illicit materials detection method using simulations and measurements with a LINAC based test bench

1) Modeling of the Varian TrueBeam® medical LINAC

As highlighted through intercomparisons of energy spectra and integrated cross-sections, the substantial lack of experimental data makes the development and validation of Monte-Carlo codes for photo-nuclear reactions very challenging. To address this critical gap, the Laboratoire National Henri Becquerel at CEA-Saclay is presently

undertaking the construction of a test bench based on a photon source produced by a medical linear electron accelerator. The chosen accelerator, a TrueBeam® model from Varian, has the capability to accelerate electrons at various energies up to a maximum of about 22 MeV.

A comprehensive geometry model of the TrueBeam® accelerator's head and its surroundings has been developed with MCNP6.2 as shown in Figure 8, enabling accurate replication of experimental conditions in Monte-Carlo simulations.

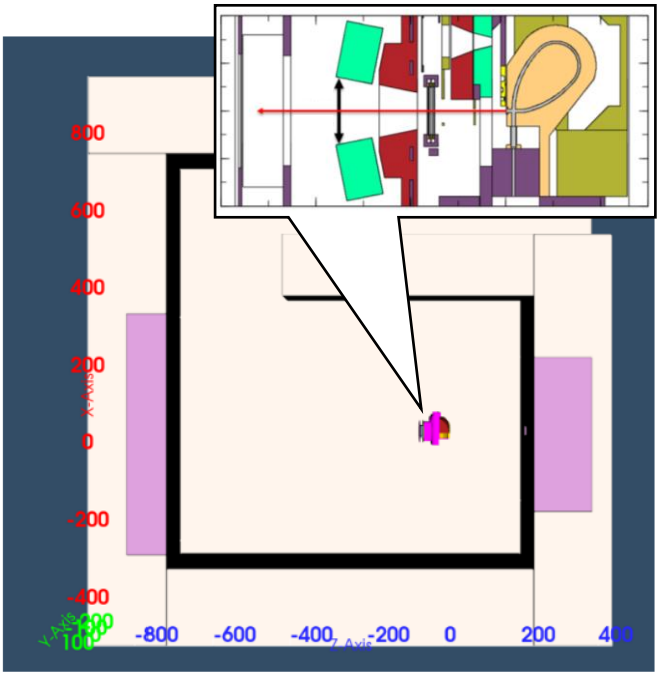

Fig. 8. Global view of the model showing the bunker of the Varian TrueBeam accelerator and a visualization of the accelerator's head geometry highlighting the level of details integrated in the simulation model.

Figure 9 is an illustration of the experimental protocol set for photo-neutron measurements. A 20 MeV electrons beam from the LINAC is stopped in the target, generating photons via the bremsstrahlung process. Subsequent interactions of photons with nuclei inside the target can occur through photo-nuclear reactions, resulting in the production of photo-neutrons. Thus, by using this optimized configuration the same target acts as producer of the photon source and as interacting media allowing photo-nuclear reactions to occur.

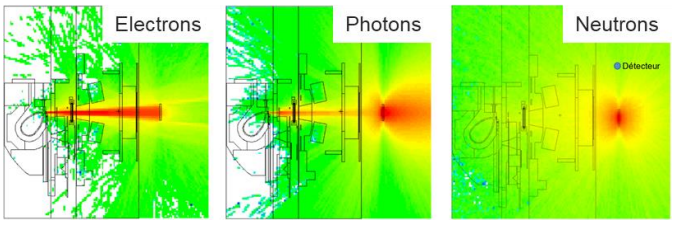

Fig. 9. Simulated electron, photon and neutron fluence maps when irradiating a 10 x 10 cm^2 wide and 1 cm thick tungsten target with a 20 MeV electron beam produced by the Varian TrueBeam® accelerator.

2) Bonner sphere based neutron spectrometry

One of the first experiments performed with the new set-up was dedicated to the measurement of photo-neutron spectrum emitted subsequent to the irradiation of a 10 x 10 cm^2 wide and 1 cm thick sample of tungsten placed at a distance of 70 cm from the beryllium vacuum window. The neutron spectrometry was conducted using a passive Bonner sphere system [14], well suited for measuring neutron spectra in pulsed and mixed n-γ fields with a strong high-energy photon component. The system comprises ten polyethylene spheres with densities of 0.95 g/cm^3. The selected sphere diameters are 7.62 cm, 8.89 cm, 10.16 cm, 11.43 cm, 12.70 cm, 15.24 cm, 17.78 cm, 20.32 cm, 25.40 cm, and 30.48 cm. Neutron detectors are placed in the center of each sphere being made of ^{197}Au foils (99.99% chemical purity, density of 19.3 g/cm^3) with a diameter of 15 mm and thickness of 0.25 mm.

The response matrix of the Bonner sphere spectrometer (BSS) was computed using MCNP6.2 simulations to cover an extended neutron energy range from 10^{-9} MeV to 20 MeV. As a result of the $^{197}Au(n,\gamma)^{198}Au$ radiative capture reaction, ^{198}Au radionuclides are created, which subsequently decay with a half-life of approximately 2.7 days through a β/γ cascade, primarily emitting 412 keV γ-rays. These γ-rays were detected and quantified using a hyper pure germanium detector (HPGe) at the LNHB activity metrology laboratory.

The specific ^{198}Au saturation activities obtained for each sphere diameter were analyzed using two custom unfolding algorithms: GRAVEL (an iteration algorithm based on SAND-II) and MLEM (a maximum likelihood expectation maximization unfolding algorithm). These unfolding algorithms are using a default spectrum, assumed to be flat in this study. In addition, a third method based on Markov chain Monte Carlo (MCMC) custom algorithm performing a Bayesian estimation of a parameterized spectrum was used to derive the final neutron spectra. The use of different unfolding algorithms allowed for the validation of results' robustness and confirmed their stability. Those algorithms were validated with the datasets given for the EURADOS comparison exercise on neutron spectra unfolding in Bonner spheres spectrometry during the 14th EURADOS Webinar [15].

Furthermore, the experimental conditions were simulated with the MCNP6.2 Monte-Carlo code using the detailed TrueBeam® geometry model described in section B-1. The calculated photo-neutron spectra were compared to the unfolded experimental spectra and the outcomes are presented in Figure 10.

As shown in the figure, the unfolded spectra using different algorithms consistently agree for neutron energies up to 6 MeV. For higher energies the agreement between GRAVEL and MLEM algorithms is preserved beyond 6 MeV, but it is essential to highlight that the shape of the neutron spectra is not physically meaningful for energies beyond around 10 MeV according to the kinetic energy constraint for primary (γ,n) reactions on natural tungsten. The continuous nature of the response matrix used by these two algorithms results in an energy spectrum artificially extended at high energies since no restriction is applied to constrain the shape of the spectrum. In contrast, the unfolded spectrum based on the MCMC method shows a trend which is more physically accurate and agreeing with the shape of the Monte-Carlo simulated photo-neutron

spectrum. However, it is important to note the significant disagreement in amplitude, as high as a factor of three, between the experimental and simulated spectra. This discrepancy has been further investigated in terms of simulation parameters to achieve improved consistency with the measurements.

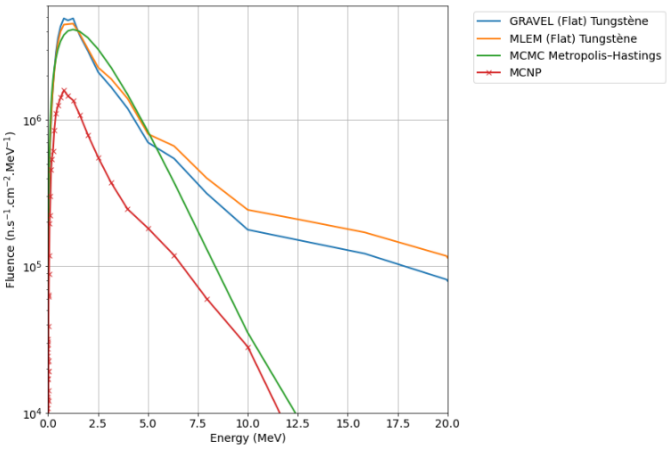

Fig. 10. Comparison between measured and simulated photo-neutron spectra from tungsten sample irradiation with 20 MeV electrons at the Varian TrueBeam® accelerator.

Consequently, additional optimization and modifications of the accelerator have been performed based on electron beam size measurements using Gafchromic® EBT-XD [16] films at a distance of 14 cm form the beryllium vacuum window. The Gafchromic® film readings are displayed in Figure 11 and allowed to conclude that, due the higher-than-expected size of the beam spot at this location, the peripheral electrons were impinging on a steel plate leading to an unwanted additional production of photons (and subsequently neutrons). This effect was not account for in the simulations which considered only the neutrons produced by the interaction of the electron beam with the tungsten sample, explaining the neutron production underestimation by the simulations observed in Figure 10.

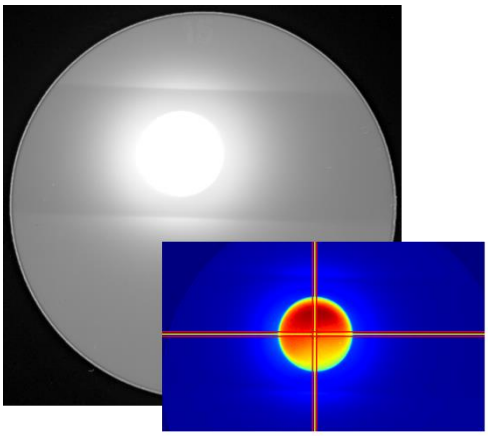

Fig. 11 Gafchromic® film signal produced by irradiation with the 20 MeV electron beam allowing to accurately measure the size of the beam spot.

Based on these findings, the configuration of the accelerator has been further optimized in order to reduce the size of the beam spot and thus to avoid additional interactions with elements other than the sample being studied. As shown in Figure 12, the electron beam spot size at the sample location (70 cm away from the beryllium vacuum window) has been decreased from the initial diameter of 29 mm to 21 mm.

Beam size measurements have been performed in addition at a distance of 14 cm, and the values obtained together with the ones measured at 70 cm allowed to calculate the divergence angle of the beam which was found to be 1.5°.

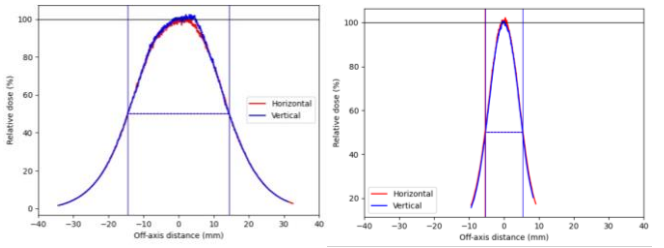

Fig. 12. Profile of the 20 MeV electron beam, before and after the modifications made to the accelerator (left and right side of the figure respectively).

With this new information in hand, an improved more accurate model of the Varian TrueBeam® accelerator for Monte-Carlo simulations has been set allowing calculations to be performed in a configuration as close as possible to the real-life experimental conditions.

These developments strongly contribute to the reliability and validity of further experiments to be performed for the establishment of an inspection method based on the active photon interrogation technique associated to the spectroscopy of photo-neutrons to be used for the detection of illicit materials.

IV. Conclusions and Perspectives

The lack of experimental energy and/or angle distributions of photo-neutrons is a serious challenge in the development and validation of Monte-Carlo codes for the simulation of applications involving photo-nuclear reactions. Current data available from the EXFOR database, which are in most cases related to total cross-section values integrated over energy and angle, does not provide enough information to rigorously test and validate the accuracy of Monte-Carlo simulations in realistically reproducing the differential distributions of photo-neutrons. This is particularly true in the case of photo-nuclear reactions on light elements, characterized by a pronounced influence of nuclear level structures on the shape of photo-neutron spectra as highlighted by the present work. Moreover, we identified significant differences when comes to the method used by the different Monte-Carlo codes tested to handle this effect, resulting in noticeable discrepancies in the results obtained namely for photo-nuclear reactions on carbon and nitrogen.

Nevertheless, our investigation revealed that very nucleus-specific, easy to identify structures in the photo-neutron spectra can serve as signatures for the detection and quantification of illicit materials containing light nuclei, such as carbon, nitrogen, or oxygen. Consequently, there is a crucial need for new measurements dedicated to experimental photo-neutron energy spectra, allowing to enhance the understanding of physics related to photo-nuclear reactions in general. This need

is strengthened by the preliminary results presented in this work, showing evidence that these specific reactions are an excellent tool in the frame of homeland security applications and that the good knowledge of the related physics is crucial in the development and optimization process.

In response, the Laboratoire National Henri Becquerel at CEA-Saclay started the construction of a test bench, based on a photon source produced by a medical linear electron accelerator and specifically optimized for photo-neutron measurements.

This pioneering setup is a major milestone as it will not only enrich the existing nuclear data on photo-nuclear reactions but will also result in a technical platform allowing to assess, optimize and finally validate the proposed innovative method for detection of illicit materials. It therefore represent a significant contribution to strengthening the reliability and accuracy of Monte-Carlo simulations when addressing photo-nuclear reactions and consequently bolstering homeland security efforts through the development of an first of its kind inspection method based on the active photon interrogation technique and the spectroscopy of photo-neutrons.

ACKNOWLEDGMENT

The authors express their gratitude to the IRSN laboratory for neutron metrology, particularly Nelson Magalotti and Quentin Ducasse, for their contributions to the neutron spectra measurements and for the loan of their passive Bonner sphere spectrometry system. Special thanks are also addressed to Marie-Christine Lepy for the support in the analysis of activated gold foils. Finally, the authors would like to acknowledge the financial support provided by the French National Laboratory of Metrology and Testing.

REFERENCES

[1] Y. Zhao, T. Cui, Y. Yang, "The design of a photo-neutron source for the narcotic drugs detection in a large-truck" in *Proc. 2017 IEEE Nuclear Science Symposium and Medical Imaging Conference (NSS/MIC 2017)*, Atlanta, Georgia, October 21–28 (2017).
[2 C. L. Fontana, A. Carnera, M. Lunardon, F. Pino, C. Sada,*et al*., "Detection system of the first rapidly relocatable tagged neutron inspection system (RRTNIS), developed in the framework of the European H2020 C-Bord project", Physics Procedia, 90, pp. 279-284 (2017).
[3] M. Gmar, E. Berthoumieux, S. Boyer, F. Carrel, D. Doré *et al*., "Detection of nuclear material by photon activation inside cargo containers", in *Proc. SPIE Defense and Security Symposium*, Orlando, Florida, April 17–21 (2006).
[4] K.W. Habiger, J.R. Clifford, R.B. Miller, W.F. McCullough, *et al*., "Explosives detection with energetic photons", *Nuclear Inst. and Methods in Physics Research B*, vol. 56-57, no. 2, pp. 834-838 (1991).
[5] The Official CERN FLUKA website, https://fluka.cern (2022).
[6 S. Agostinelli, J. Allison, K. Amako, J. Apostolakis, H. Araujo, *et al*., « GEANT4—a simulation toolkit », *Nuclear Inst. and Methods in Physics Research A*, vol. 506, no.3, pp. 250–303 (2003).
[7] C. J. Werner, MCNP users manual - code version 6.2, LA-UR-17-29981.
[8] T. Sato,Y. Iwamoto, S. Hashimoto, T. Ogawa, T. Furuta, *et al*., "Features of particle and heavy ion transport code system (PHITS3.27) version 3.02", *Journal of Nuclear Science and Technology,* vol. 55, no. 6, pp. 684–690 (2018).
[9] N. Otuka, B. Pritychenko, N. Otuka, E. Dupont, V. Semkova, *et al*., "Towards a More Complete and Accurate Experimental Nuclear Reaction Data Library (EXFOR): International Collaboration Between Nuclear Reaction Data Centres (NRDC)", *Nucl. Data Sheets*, vol. 120, no. 272 (2014).
[10] A. Koning, D. Rochman, "Modern nuclear data evaluation with the TALYS code system", *Nuclear Data Sheets,* vol. 113, no. 2841 (2012).
[11] B. C. Cook, J. E. E. Baglin, J. N. Bradford, J. E. Griffin, "^{12}C (γ,n) ^{11}C Cross Section to 65 MeV", *Phys. Rev*. vol. 143, no. 724 (1966).
[12] B. L. Berman, S. C. Fultz, J. T. Caldwell, M. A. Kelly, S. S. Dietrich, "Photoneutron Cross Sections for Ba-138 and N-14", *Phys. Rev. C,* vol. 2, no. 2318 (1970).
[13] J. D. King, R. N. H. Haslam, R. W. Parsons, "The gamma-neutron cross section for N-14", *Canadian Journal of Physics*, vol. 38, no. 2 (1960).
[14] K. Amgarou, V. Lacoste, A. Martin, B. Asselineau, L. Donadille, "Neutron Spectrometry With a Passive Bonner Sphere System Around a Medical LINAC and Evaluation of the Associated Unfolding Uncertainties", *IEEE Transactions on Nuclear Science*, vol. 56 no. 5, pp. 2885-2895 (2009).
[15] J. M. Gómez-Ros, R. Bedogni, C. Domingo, J. S. Eakins, N. Roberts, *et al*., "International comparison exercise on neutron spectra unfolding in bonner spheres spectrometry: problem description and preliminary analysis", *Radiation Protection Dosimetry*, vol. 180, no. 1-4, pp. 70–74 (2018).
[16] http://www.gafchromic.com/